LJMU Research Online

Alfagih, IM, Kunda, NK, Alanazi, F, Dennison, SR, Somavarapu, S, Hutcheon, GA and Saleem, IY

 Pulmonary Delivery of Proteins Using Nanocomposite Microcarriers.

http://researchonline.ljmu.ac.uk/id/eprint/2299/

Article

For more information please contact researchonline@ljmu.ac.uk

Pulmonary Delivery of Proteins Using Nanocomposite Microcarriers

IMAN ALFAGIH,[1,2] NITESH KUNDA,[1] FARES ALANAZI,[3] SARAH R. DENNISON,[4] SATYANARAYANA SOMAVARAPU,[5]
GILLIAN A. HUTCHEON,[1] IMRAN Y. SALEEM[1]

[1]School of Pharmacy and Biomolecular Sciences, Liverpool John Moores University, Liverpool, UK

[2]Department of Pharmaceutics, King Saud University, Riyadh, Saudi Arabia

[3]Kayali Chair for Pharmaceutical Industries,Department of Pharmaceutics, King Saud University, Riyadh, Saudi Arabia

[4]Research and Innovation, University of Central Lancashire, Preston, UK

[5] UCL School of Pharmacy, London, UK

ABSTRACT: In this study, Taguchi design was used to determine optimal parameters for the preparation of bovine serum albumin (BSA)-loaded nanoparticles (NPs) using a biodegradable polymer poly(glycerol adipate-co-ω-pentadecalactone) (PGA-co-PDL). NPs were prepared, using BSA as a model protein, by the double emulsion evaporation process followed by spray-drying from leucine to form nanocomposite microparticles (NCMPs). The effect of various parameters on NP size and BSA loading were investigated and dendritic cell (DC) uptake and toxicity. NCMPs were examined for their morphology, yield, aerosolisation, *in vitro* release behaviour and BSA structure. NP size was mainly affected by the polymer mass used and a small particle size $\leq$500 nm was achieved. High BSA (43.67 $\pm$ 2.3 μg/mg) loading was influenced by BSA concentration. The spray-drying process produced NCMPs (50% yield) with a porous corrugated surface, aerodynamic diameter 1.46 $\pm$ 141 μm, fine particle dose 45.0 $\pm$ 4.7 μg and fine particle fraction 78.57 $\pm$ 0.1%, and a cumulative BSA release of 38.77 $\pm$ 3.0% after 48 h. The primary and secondary structures were maintained as shown by sodium dodecyl sulphate poly (acrylamide) gel electrophoresis and circular dichroism. Effective uptake of NPs was seen in DCs with >85% cell viability at 5 mg/mL concentration after 4 h. These results indicate the optimal process parameters for the preparation of protein-loaded PGA-co-PDL NCMPs suitable for inhalation. © 2015 Wiley Periodicals, Inc. and the American Pharmacists Association J Pharm Sci

Keywords: nanoparticles; biodegradable polymers; polymeric drug delivery systems; particle size; pulmonary delivery; protein delivery and formulation; spray-drying

INTRODUCTION

Pharmaceutical research has recently focussed on developing delivery systems for macromolecules such as proteins, peptides and antigens as they become the preferred therapeutics because of their greater selectivity, lower disruption of normal biological processes and reduced clinical development time with a shorter United States Food and Drug Administration approval period.[1] However, to reach a therapeutic level most of these macromolecules must be administered repeatedly in an invasive manner.[2] The pulmonary delivery of macromolecules is a viable alternative because of the attractive physiological properties of the lungs; the pulmonary epithelium is more permeable and lower enzymatic activity than the gut. In addition, it has a large surface area that is highly vascularised with thin epithelium in the alveolar lung tissue.[3] In addition, the pulmonary epithelium has many immunological properties.[2] Most organisms causing respiratory infections attack the host via the mucosal membrane. Consequently, the non-invasive pulmonary delivery of antigens can provide protection to mucosal membranes at the site of infection and potentially provides a first-line defense against invading microorganism.[4] The extensive dendritic cell (DC) networks that line the respiratory epithelium are considered an ideal target to initiate a strong immune response.[2] Moreover, pulmonary delivery reduces the risk of cross contamination due to the reuse of needles and syringes, and eliminates needle stick injuries, in both patients and medical personnel.[4]

Nanoparticles (NPs) are a useful delivery system for pulmonary macromolecules because of their potential for targeted drug delivery, sustained release and reduced dosing frequency, hence improving patient compliance and convenience.[5] They provide an additional advantage for antigen delivery systems, with studies suggesting NPs of about 500 nm or less were optimal for DCs uptake.[6,7] A most common method for the encapsulation of water-soluble drugs such as protein, peptides and antigens in biodegradable polymer-based NPs is the water-oil-water (w/o/w) double-emulsion solvent evaporation method.[2] Biodegradable poly(glycerol adipate-co-ω-pentadecalactone, PGA-co-PDL) has previously been investigated as a novel delivery system of small molecule, for example, dexamethasone phosphate,[8] model drugs, for example,

ibuprofen[9] and sodium fluorescein,[10] and macromolecules, for example, DNase I,[11] via dry powder inhalation (DPIs). However, particles smaller than 1 µm show poor lung deposition and are likely to be exhaled because of their low inertia, whereas particles larger than 5 µm cannot pass the oropharynx effectively.[12] Hence, to achieve particle deposition in the respirable region of the lung, the particles should be in the size range 1–5 µm. NPs can be formulated into microparticle carriers with an aerodynamic diameter between 1 and 5 µm to form nanocomposite microparticles (NCMPs) as DPIs by spray-drying.[13–16]

Spray-drying is a process where the formulation is presented as a feed solution, suspension or emulsion and converted into fine droplets, followed by exposure to rapid hot air-stream resulting in dry respirable-sized powders. In addition to the composition of the feed formulation, several operational parameters greatly affect the quality and quantity of the final formulation such as inlet temperature, air flow, aspiration capacity and feed rate.[17–20] Biocompatible excipients (carbohydrates, amino acids and lipids) are typically added to the formulation feed to afford dry powders with bulk and to promote the production of a desirable aerodynamic particle size which upon inhalation allows rapid release of NPs in the lung fluid.[10,13,17,21–23] In addition, the excipients can protect the NPs and encapsulated agents against the extreme spray-drying process conditions such as high temperatures and shear forces.[24] Delivering these microparticle carriers as DPIs via the pulmonary route offer many advantages such as not requiring trained medical personnel, eliminates cold-chain requirements and offers increased physical and chemical stability of macromolecules in comparison with liquid formulations.[4]

The Taguchi design is a useful method for studying a large number of parameters and interactions as it has the ability to optimise many parameters simultaneously and extract quantitative data from only a few experiments compared with the traditional factorial design.[25,26] For example, a single replicate of four parameters and three level experiments would require 81 runs for a full factorial analysis. However, using the Taguchi method will require only nine runs. The Taguchi approach has previously been used in the improvement of dosage forms.[25] Moreover, the Taguchi design concentrates on product robustness against uncontrollable (noise) factors. It employs a signal-to-noise (S/N) ratio to quantify variations. These ratios are meant to be used as measures of the effect of noise (uncontrollable) factors on performance characteristics. S/N ratios take into account both amount of variability in response data and closeness of average response to the target (1). In Taguchi design, S/N ratio can be defined as the measure of the deviation of the response from the desired value. So, 'signal' presents the mean value and 'noise' presents the SD. It means that lower variability in the process is ensured through maximising the S/N ratio (2). The variability of a characteristic is due to the noise factor such as environmental factors. Thus, optimising process parameters by the Taguchi design leads to bringing the average quality near to the target value, and also to simultaneously decrease the variation in quality (3). The experimental condition having the maximum S/N ratio is considered the optimum condition, as the variability of characteristics is in inverse proportion to the S/N ratio (4).

In this study, we have formulated PGA-co-PDL NPs encapsulating bovine serum albumin (BSA), a model protein, using Taguchi design to optimise NPs size and drug loading (DL) for effective uptake by DCs. The PGA-co-PDL NPs were then incorporated into L-leucine microparticle carriers via spray-drying using condition optimised using Taguchi design to produce NCMPs carriers suitable for pulmonary delivery via DPIs, maintaining BSA structure and activity.

MATERIALS AND METHODS

Materials

Poly(glycerol adipate-co-ω-pentadecalactone) (MW of 16.7 kDa) polymer was synthesised and characterised in our laboratory as previously described by Thompson et al.[27] BSA was obtained from (MW 67 kDa) Avenchem, UK. Poly(vinyl alcohol) (PVA; MW of 13–23 kDa, 87%–89% hydrolysed) was obtained from Clariant GmbH, Frankfurt, Germany. Dichloromethane (DCM) was purchased from BDH, Laboratory Supplies, UK. QuantiPro bicinchoninic acid (BCA) protein assay kit, L-leucine, phosphate buffer saline tablet (PBS; pH 7.4), 3-(4,5-dimethylthiazol-2-yl)-2,5-diphenyltetrazolium bromide (MTT), RPMI-1640 medium with L-glutamine and sodium hydrogen carbonate (NaHCO$_3$), tween 80, albumin tagged with fluorescein isothiocyanate (FITC-BSA) were purchased from Sigma–Aldrich, UK. Minimum essential medium (MEM) alpha-nucleosides were obtained from Gibco by Life Technologies, UK. 75 cm^2/tissue culture flask (vented cap), 96-well flat bottom plates, acetone, antibiotic/antimyotic solution (100×), dimethyl sulfoxide (DMSO) and paraformaldehyde were purchased from Fisher Scientific, UK. CVS10D omniPAGE vertical gel electrophoresis system, protoGel stacking buffer, protein molecular weight markers in the range 10–220 kDa, protein loading buffer blue (2×) [0.5 M Tris–HCl (pH 6.8), 4.4% (w/v) SDS, 20% (v/v) glycerol, 2% (v/v) 2-mercaptoethanol and bromphenol blue in distilled/deionised water], Tris–glycine–sodium dodecyl sulphate-polyacrylamide gel electrophoresis (SDS-PAGE) buffer (10×) containing 0.25 M Tris base, 1.92 M glycine and 1% (w/v) SDS were purchased from Geneflow Limited, UK. 4-Nitrophenyl acetate esterase substrate (NPAES) was purchased from Sigma–Aldrich. Heat inactivated foetal calf serum (FCS) was purchased from Biosera, UK. Adenocarcinomic human alveolar basal epithelial cell line, A 549 (CCL-185TM) and immature DCs; monocyte, mouse, JAWS II (CRL-11904TM) were purchased from American Type Culture Collection (ATCC); 4′,6-diamidino-2-phenylindole, dihydrochloride (DAPI) and Wheat Germ Agglutinin Texas RedR-X conjugate (WGA TR) were purchased from Invitrogen, Ltd., UK.

Experimental Design and NP Preparation

Taguchi design L36 orthogonal array was constructed through Minitab 16 Statistical Software® (Minitab Inc., Pennsylvania). It was composed of eight variables set at two levels or three levels (Table 1). This design was used to identify the important parameters that would influence the NP size and BSA loading. A high signal-to-noise (S/N) ratio indicated the optimum conditions. The signal factor (S) was the outcome, that is, particle size or BSA loading and noise factors (N) included room temperature, humidity, experience of researcher and so on. Optimisation of the particle size and BSA loading was performed using the Taguchi's 'smaller-is-better' and 'larger-is-better' criterion, respectively.[28]

Bovine serum albumin-loaded PGA-co-PDL NPs were prepared using a (w/o/w) double emulsion/solvent evaporation method. Briefly, BSA solution containing PVA (internal aque-

Table 1. Double Emulsion Solvent Evaporation Processing Variables, Units and Levels for BSA-Loaded PGA-co-PDL NPs

Code	Variables	Unit	Levels		
			1	2	3
A	IAP volume	mL	0.25	0.5	–
B	OP volume	mL	1	2	–
C	BSA concentration	%	50	100	200
D	Polymer mass	mg	50	100	200
E	PVA concentration	%	1	5	10
F	Sonication time IAP	s	5	10	15
G	Sonication time EAP	s	10	15	30
H	Sonication amplitude	%	30	45	65

IAP, internal aqueous phase; OP, organic phase; EAP, external aqueous phase.

ous phase, IAP) was emulsified in DCM (organic phase, OP) containing PGA-co-PDL, using a probe sonicator (VC X 500 Vibra-Cell™; Sonics & Materials, Inc., Newtown, Connecticut; 13 mm probe) over an ice bath. The resulting single emulsion was emulsified into 25 mL of a PVA solution (1%, w/v) (external aqueous phase, EAP) using the same probe sonicator to form a w/o/w double emulsion. The DCM was evaporated by magnetically stirring the double emulsion for 2 h at room temperature. The NPs were collected by centrifugation (Sigma 3–30k; SIGMA Laborzentrifugen GmbH, Germany) at 40,000*g* for 1 h at 4°C, and washed twice with distilled water. Control NPs were prepared using the same method without BSA.

Experimental Design and NCMPs Preparation

A second design was constructed using an L27 orthogonal array design through Minitab 16 Statistical Software® (Minitab Inc.). It composed of five variables each set at three levels (Table 2). Optimisation of yield% was undertaken using the Taguchi's 'larger-is-better' criterion.

Spray-drying was used to incorporate the PGA-co-PDL NPs into NCMPs using L-leucine as a carrier. NPs (control and BSA loaded) were suspended in an aqueous L-leucine solution at a polymer-to-carrier ratio of 1:1.5 (w/w) and spray-dried with a Büchi B-290 mini-spray dryer (Büchi Labortechnik, Switzerland) containing a standard two-fluid nozzle (0.7 mm diameter). The dried powder (PGA-co-PDL/L-leucine NCMPs) was separated from the air stream using a high-performance cyclone (Büchi Labortechnik), collected and stored in a desiccator at room temperature prior to further investigations.

NP Characterisation

Particle Size, Polydispersity Index and Zeta Potential.

Samples were analysed by laser diffraction (Zetasizer Nano ZS; Malvern Instruments Ltd., UK). Briefly, 200 µL aliquot of the double emulsion sample was diluted with deionised water (8 mL), and placed into a cuvette with the measurements conducted at ambient temperature (25°C) ($n = 3$).

Protein Loading of NPs.

The amount of protein loaded in the NPs was determined by measuring the amount of protein remaining in the supernatant and wash after centrifugation using a QuantiPro BCA protein assay kit ($n = 3$), by UV spectroscopy at 562 nm (Genesys 5 spectrophotometer; Thermo Fisher Scientific Inc., Waltham, Massachusetts). A calibration curve was obtained with BSA standard solutions (2.5–30 µg/mL) and the DL was calculated

according to Eq. 1:

$$DL = \frac{\text{actual amount of encapsulated BSA} (\mu g)}{\text{actual amount of nanoparticles} (mg)} \quad (1)$$

NCMPs Characterisation

Particle Size and Morphology.

To ensure the recovery of NPs from NCMPs, 5 mg of NCMPs was suspended in 10 mL deionised water and measurements performed as described in section 1.5.1 ($n = 3$). **Q3**

Scanning electron microscopy (SEM) (FEI—Quanta™ 200 ESEM, Holland) was used to visualise the morphology of NCMPs. Spray-dried NCMPs samples were placed on aluminium stubs (pin stubs, 13 mm) covered with a conductive carbon tab and coated (EmiTech K 550X Gold Sputter Coater, 25 mA) with palladium (10–15 nm) for 3 min.

Yield of Spray-Dried NCMPs.

The percentage yield of dry powder NCMPs was calculated as the mass of expected total powder ($n = 3$) according to Eq. 2:

$$\%\text{Yeild} = \frac{\text{Weight of powder collected after spray drying}}{\text{Weight of total dry mass used for the preparation}} \times 100 \quad (2)$$

Moisture Content.

Thermogravimetric analysis (TGA Q50, UK equipped with TA universal analysis 2000 software) was used to evaluate the moisture content of dry powder NCMPs after spray-drying. Approximately 10–15 mg of NCMPs was placed in a platinum pan and heated between 25°C and 650°C at a purged with nitrogen at 20 mL/min and a scanning rate at 10°C/min. The moisture content was analysed for data collected between 25°C and 120°C.

Powder Density and Primary Aerodynamic Diameter.

The tapped density of selected NCMPs was determined by inserting approximately 0.2 g of powder into a 5 mL graduated cylinder and recording the initial volume. Tapped density measurements were then performed until no change in volume was observed ($n = 3$). The data obtained from geometric particle size (d) and tapped density (ρ) was used to determine the theoretical aerodynamic diameter (d_{ae}) according to Eq. 3.

$$d_{ae} = d \sqrt{\frac{\rho}{\rho_1}}_{\rho_1 = 1 \text{ g/cm}^3} \quad (3)$$

Table 2. Spray-Drying Processing Variables, Units and Levels for BSA-Loaded PGA-co-PDL NCMPs

Code	Variable	Unit	Level		
			1	2	3
A	Air flow	L/h	400	535	670
B	Inlet temp	C	50	75	100
C	Aspirator	%	50	75	100
D	Feed rate	%	5	10	15
E	Concentration	mg/mL	12.5	6.25	4.17

In Vitro Aerosolisation Investigations.

The aerosolisation studies of the NCMPs were evaluated using the next-generation impactor (NGI). Optimum NCMPs formulations ($n = 3$) were filled into capsules (hydroxypropyl methylcellulose, size 3. 4 capsules each corresponding to 10 mg spray-dried powder) and aerosolised via a Cyclohaler® (Teva Pharma) into NGI. The capsules were punctured using the actuator of the Cyclohaler® prior to inhalation at a flow rate of 60 L/min for 4 s.[29] The samples were collected using DCM/0.15 M NaCl mixture (2:1) to extract the BSA from the polymer, which was then analysed by the QuantiPro BCA protein assay as mentioned above. The fine particle dose (FPD) was determined as the total mass of powder deposited in NGI stages with aerodynamic diameters less than 4.5 µm, the fine particle fraction (FPF%) was determined as the fraction of emitted dose deposited in the NGI with aerodynamic diameters less than 4.5 µm, and the mass median aerodynamic diameter (MMAD) was calculated from log-probability analysis.

In Vitro Release Studies.

Nanocomposite microparticles samples (10 mg) were placed in microtubes and dispersed in 1.2 mL of PBS (pH 7.4), and incubated at 37°C, rotating at 20 RPM in a sample mixer (HulaMixer, Invitrogen Dynal AS, Life Technologies). At predetermined time intervals up to 48 h, samples were centrifuged (13,000 rpm for 30 min) and 0.5 mL of the supernatant removed and replaced with fresh buffer. The supernatant was analysed by QuantiPro BCA protein assay as mentioned above ($n = 3$). The percentage cumulative BSA released was calculated according to Eq. 4.

$$\%\text{Cumulative protein released}$$
$$= \frac{\text{cumulative protein released}}{\text{actual protein loaded}} \times 100 \qquad (4)$$

The % cumulative protein release was assessed using zero order, first order and Higuchi's square root plot release models.[30] The correlation coefficient was calculated from the following graphical representations, zero order: % cumulative protein release versus time; first order: log% cumulative protein remaining versus time; Higuchi: % cumulative protein release versus square root of time.

Protein Characterisation

Sodium Dodecyl Sulphate-Polyacrylamide Gel Electrophoresis.

The primary structure of released BSA from NPs and NCMPs was characterised by SDS-PAGE performed on a CVS10D omniPAGE vertical gel electrophoresis system with 9% stacking gel prepared using ProtoGel stacking buffer containing 0.4% of SDS. Protein samples and standard were treated with protein loading buffer blue (2×) (0.5 M Tris–HCl (pH 6.8), 4.4% (w/v) SDS, 20% (v/ v) glycerol, 2% (v/v) 2-mercaptoethanol and bromphenol blue in distilled/deionised water) in a ratio 1:1 (v/v) buffer-to-sample for 3 min at 95°C. The protein molecular weight marker, standard and samples were loaded into the wells (25 µL per well). Electrophoresis was performed with Tris–glycine–SDS-PAGE buffer (10×) [0.25 M Tris base, 1.92 M glycine, 1% (w/v) SDS] at a constant voltage of 100 V for 2.3 h. Coomassie Brilliant Blue was used to stain the gel followed by destaining in distilled water for 24 h. Gel scanner (GS-700 Imaging Densitometer; Bio-Rad) equipped with Quantity One software was used for the gel imaging and documentation.

Circular Dichroism.

The secondary structure of standard BSA (as a control), and BSA released after 48 h from NCMPs in PBS was determined via circular dichroism (CD) using a J-815 spectropolarimeter (Jasco, UK) at 20°C as reported previously.[31] Five scans were recorded per sample using a 10 mm path-length cells at far-UV wavelengths from 260 to 180 nm at a data pitch of 0.5 nm, band width of 1 nm and a scan speed 50 nm/min. Far-UV CD spectra were collated for standard BSA and BSA released in PBS after 48 h, and the baseline acquired without the sample was subtracted.[32] The secondary structure of the samples was estimated using the CDSSTR method[33] protein reference set 3 from the DichroWeb server.[34,35]

Determination of BSA Activity.

A freshly prepared NPAES solution[36] (15 µL of a 5 mM solution in acetonitrile) was added to the released BSA sample (1.2 mL in PBS, 50 µg/mL) and incubated for 1 h (HulaMixer™ Sample Mixer). The absorbance of the sample mixture was measured at 405 nm with standard BSA (50 µg/mL) used as a positive control and PBS buffer alone as a negative control. The BSA relative residual esterolytic activity was determined as the ratio of absorbance between the released BSA to standard BSA. The esterolytic activity for standard BSA was considered as 100%.

Cell Viability Studies.

A549 cells were cultured in RPMI-1640 medium containing 10% FCS/1% antibiotic/antimycotic solution (complete growth medium—i). DCs were cultured in MEM alpha medium containing ribonucleosides, deoxynucleosides, 4 mM L-glutamine, 1 mM sodium pyruvate 2 mM, supplemented with 20% FCS, 5 ng/mL murine growth GM-CSF and 1% antibiotic/antimycotic solution (complete growth medium—ii).

The toxicity profiles of NPs and NCMPs were assessed over 24 h in A549 and of NPs only over 4 h in DCs using MTT assay. Cells were cultured in 96-well plates with 100 µL

(2.5 × 10^5 cells/mL) complete growth medium i and ii, respectively, at 37°C and 5% CO_2. Then, complete growth medium (100 µL) containing NPs (0–5 mg/mL) ($n = 3$) and 10% DMSO as a positive control were added to the wells and incubated for a further 4 h with DCs or with NPs and NCMPs (0–1.25 mg/mL) ($n = 3$) for 24 h in A549 cells. This was followed by the addition of 40 µL MTT solution (5 mg/mL in PBS, pH 7.4) to each well and incubated for 2 h. The medium was then gently removed (for DCs the 96-well plate was centrifuged at 1300g for 7 min at 4°C to pellet the suspended cells), and any formazan crystals generated were solubilised with 100 µL of DMSO and the absorbance measured using a microplate reader (Epoch, BioTek Instruments Ltd., UK) at 570 nm. The % cell viability was calculated as the absorbance ratio between NPs or NCMPs-treated and untreated control cells.

In Vitro NPs Uptake into DCs.

Dendritic cells uptake of FITC-BSA NPs was visualised using confocal laser scanning microscopy (CLSM) (Carl Zeiss lsm 710, UK) and image analysis was performed using Zeiss LSM software The DCs (2 × 10^5 cells/400 µL) were plated into an eight-well chambered borosilicate cover glass system, and incubated at 37°C and 5% CO_2 for 48 h prior to treatment with NPs. The FITC-BSA NPs (40 µg/40 µL) were placed in the wells and incubated as above for 1 h. The suspensions from each well were removed and washed using PBS. Cells were fixed for 15 min with 300 µL of 4% paraformaldehyde in PBS followed by washing with PBS. The cell membranes were counterstained with WGA TR and the nuclei were counterstained with DAPI added to each well and incubated as above for 10 min, followed by washing with PBS. The cells were examined using a CLSM placed on a computer-controlled inverted microscope (Axiovert 200 M BP). Cells were imaged by excitation at a wavelength of 595 nm (red channel for WGA TR), 358 nm (blue channel for DAPI), 488 nm (green channel for FITC-BSA), with a Plan Neofluar 63×/0.30 numerical aperture objective lens.

Statistical Analysis.

Minitab 16 Statistical Software® (Minitab Inc.) was employed for all statistical analysis and graph plotting. The data obtained were analysed statistically by one-way ANOVA with the Tukey's comparison using Minitab 17.1 Statistical Software® (Minitab Inc.). Statistical significant difference was noted when $p < 0.05$. Data are stated as the mean ± SD.

RESULTS

Optimisation of the BSA-Loaded NPs using Taguchi Design

The Taguchi L_{36} orthogonal array design required 36 runs to be performed to ascertain the important factors influencing the NP size and DL and to produce the optimum conditions for each variable to achieve the smallest particle size NPs (SPS NPs), and highest DL NPs (HDL NPs). Table 3 shows the L_{36} orthogonal array and the measured NP size and DL. Analysis of the results indicated particle sizes ranging from 216.2 ± 39.9 to 2168.9 ± 1553 nm and DL ranging from 0.8 ± 0.6 to 26.8 ± 5.8 µg/mg were obtained (Table 3).

Figures 1 and 2 show the mean S/N graph of the NP size and DL of BSA, respectively, for each parameter level. The factor with the largest range and corresponding rank (indicating the
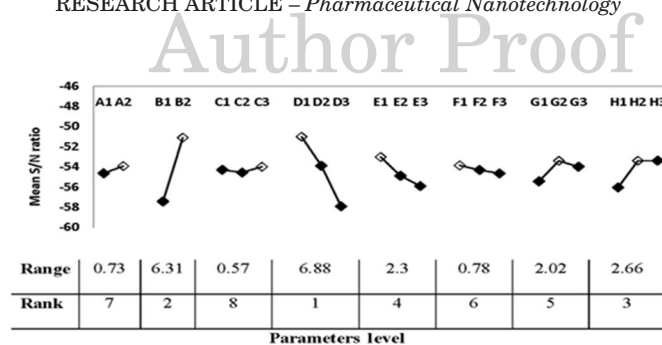
Figure 1. Mean signal-to-noise (S/N) graph for particle size response. Letters (A–H) indicate the experimental parameters and numeric value indicates the parameter levels, ◊ indicates maximum S/N value. A, IAP volume; B, OP volume; C, BSA concentration; D, polymer mass; E, PVA concentration; F, IAP sonication time; G, EAP sonication time; H, sonication amplitude.
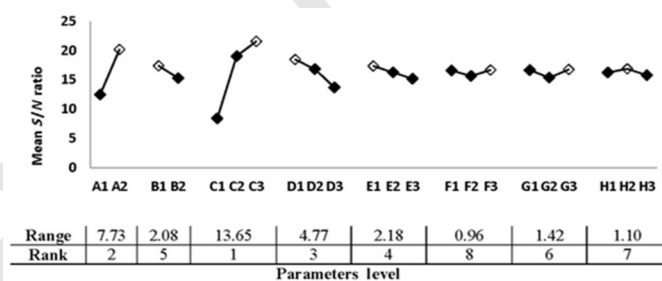
Figure 2. Mean signal-to-noise (S/N) graph for BSA loading response. Letters (A–H) indicate the experimental parameters and numeric value indicates the parameter levels, ◊ indicates maximum S/N value. A, IAP volume; B, OP volume; C, BSA concentration; D, polymer mass; E, PVA concentration; F, IAP sonication time; G, EAP sonication time; H, sonication amplitude.

relative importance compared with other factors) was considered as the significant factor influencing the size or DL.

The optimum conditions, based on the range, rank and S/N graph (Fig. 1), for producing SPS NPs according to the Taguchi's 'smaller-is-better' criterion in Minitab® 16 statistical software was A2B2C3D1E1F1G2H2. When this optimised run was performed the measured particle size obtained was 203.0 ± 5.4 nm, which was lower than the minimum particle size of 216.2 ± 39.9 nm prepared using run 29. It is also worth mentioning that the measured BSA loading of SPS NPs was 35.9 ± 2.4 µg/mg. For the production of HDL NPs (Fig. 2) using the Taguchi's 'larger-is-better' criterion, the optimal conditions were A2B1C3D1E1F3G3H2 which produced a DL of 43.67 ± 2.3 µg/mg. This was higher than the maximum DL of 26.8 ± 5.8 µg/mg obtained using run 24. The particle size of HDL NPs was 287 ± 24.4 nm.

Optimisation of the Spray-Drying Process using Taguchi Design

Spray-drying was employed to encompass selected NP formulations into NCMPs using L-leucine as a carrier and to enhance powder dispersion. The Taguchi L27 orthogonal array design required 27 runs to be performed to produce the optimum condition for each factor to achieve the highest yield % of dry powder. Table 4 shows the structure of the Taguchi L27 orthogonal array design and the measured dry powder yield % which ranged from no yield to 49.8 ± 0.2%.

Table 3. The Experimentally Measured Values of Particle Size (PS), Polydispersity Index (PI) and Drug Loading (DL) of NPs

Run	A	B	C	D	E	F	G	H	PS (nm)	PI	DL (µg/mg)
1	1	1	1	1	1	1	1	1	574.4 ± 120.6	0.395 ± 0.15	3.6 ± 0.2
2	1	1	2	2	2	2	2	2	648.5 ± 10.5	0.209 ± 0.1	6.9 ± 0.4
3	1	1	3	3	3	3	3	3	1165.9 ± 337.9	0.181 ± 0.2	7.0 ± 0.1
4	1	1	1	1	1	1	2	2	498.7 ± 4.6	0.311 ± 0.01	2.4 ± 0.4
5	1	1	2	2	2	2	3	3	1032.9 ± 41.9	0.185 ± 0.3	5.7 ± 0.5
6	1	1	3	3	3	3	1	1	1534.7 ± 1484.0	0.172 ± 0.2	4.9 ± 3.4
7	1	1	1	1	2	3	1	2	577.8 ± 107.4	0.236 ± 0.1	4.1 ± 0.6
8	1	1	2	2	3	1	2	3	550.4 ± 93.9	0.146 ± 0.2	4.6 ± 0.9
9	1	1	3	3	1	2	3	1	1836.4 ± 864.0	0.273 ± 0.2	9.3 ± 0.2
10	1	2	1	1	3	2	1	3	357.5 ± 102.0	0.159 ± 0.03	0.8 ± 0.6
11	1	2	2	2	1	3	2	1	349 ± 68.9	0.124 ± 0.1	6.4 ± 0.9
12	1	2	3	3	2	1	3	2	325 ± 73.3	0.162 ± 0.03	4.3 ± 0.9
13	1	2	1	2	3	1	3	2	270.8 ± 81.0	0.133 ± 0.004	1.4 ± 0.5
14	1	2	2	3	1	2	1	3	416.4 ± 100.8	0.083 ± 0.1	3.9 ± 0.3
15	1	2	3	1	2	3	2	1	319.7 ± 41.9	0.142 ± 0.002	5.0 ± 4.0
16	1	2	1	2	3	2	1	1	493.1 ± 36.1	0.243 ± 0.06	1.9 ± 0.2
17	1	2	2	3	1	3	2	2	443.6 ± 47.0	0.135 ± 0.1	4.3 ± 0.2
18	1	2	3	1	2	1	3	3	230.7 ± 46.7	0.100 ± 0.01	15.7 ± 4.8
19	2	1	1	2	1	3	3	3	420.8 ± 75.9	0.081 ± 0.1	5.0 ± 0.1
20	2	1	2	3	2	1	1	1	1375.8 ± 392.2	0.005 ± 0	7.1 ± 0.1
21	2	1	3	1	3	2	2	2	467.3 ± 104.4	0.005 ± 0	19.2 ± 5.9
22	2	1	1	2	2	3	3	1	1204.7 ± 450.6	0.342 ± 0.1	5.6 ± 0.04
23	2	1	2	3	3	1	1	2	2168.9 ± 1553.0	0.003 ± 0.002	20.4 ± 0.7
24	2	1	3	1	1	2	2	3	267 ± 10.2	0.061 ± 0.07	26.8 ± 5.8
25	2	1	1	3	2	1	2	3	554.1 ± 88.7	0.111 ± 0.09	2.8 ± 0.1
26	2	1	2	1	3	2	3	1	468.2 ± 50.0	0.005 ± 0.0	15.8 ± 0.3
27	2	1	3	2	1	3	1	2	493.1 ± 104.0	0.046 ± 0.05	24.5 ± 3.1
28	2	2	1	3	2	2	2	1	535.1 ± 3.4	0.175 ± 0.1	2.7 ± 0.02
29	2	2	2	1	3	3	3	2	216.2 ± 39.9	0.104 ± 0.04	15.5 ± 0.9
30	2	2	3	2	1	1	1	3	343.4 ± 54.3	0.194 ± 0.03	17.7 ± 1.2
31	2	2	1	3	3	3	2	3	729.9 ± 54.6	0.269 ± 0.05	2.2 ± 0.4
32	2	2	2	1	1	1	3	1	246.5 ± 32.2	0.103 ± 0.02	18.8 ± 1.2
33	2	2	3	2	2	2	1	2	316.7 ± 59.8	0.212 ± 0.02	18.1 ± 0.1
34	2	2	1	3	1	2	3	2	430.1 ± 207.8	0.233 ± 0.1	3.1 ± 0.2

Table 3. Continued

Run	A	B	C	D	E	F	G	H	PS (nm)	PI	DL (μg/mg)
35	2	2	2	1	2	3	1	3	301.5 ± 19.6	0.095 ± 0.12	21.5 ± 1.9
36	2	2	3	2	3	1	2	1	463.5 ± 123.4	0.246 ± 0.03	19.2 ± 2.1
SPS	2	2	3	1	1	1	2	2	203.0 ± 5.4	0.201 ± 0.03	35.9 ± 2.4
HDL	2	1	3	1	1	3	3	2	287.0 ± 24.4	0.122 ± 0.05	43.7 ± 2.3

Data represent as mean $\pm$ SD, $n = 3$.
Note: A, IAP volume; B, organic phase volume; C, BSA concentration; D, polymer mass; E, PVA concentration; F, sonication time IAP; G, sonication time EAP; H, sonication amplitude; DL, BSA loading; SPS, smallest particle size NPs; HDL, highest drug loading NPs.

Table 4. Spray-Drying Processing Variables for NCMPs Using Taguchi Design and Corresponding Yield%

Runs	A	B	C	D	E	Yield (%)
1	1	1	1	1	1	34.1 ± 2.2
2	1	1	1	1	2	30.5 ± 4.5
3	1	1	1	1	3	27.8 ± 0.3
4	1	2	2	2	1	26.5 ± 3.9
5	1	2	2	2	2	37.7 ± 0.7
6	1	2	2	2	3	29.4 ± 7.9
7	1	3	3	3	1	43.1 ± 2.4
8	1	3	3	3	2	41.9 ± 2.1
9	1	3	3	3	3	37.0 ± 1.0
10	2	1	2	3	1	0
11	2	1	2	3	2	0
12	2	1	2	3	3	0
13	2	2	3	1	1	49.8 ± 0.2
14	2	2	3	1	2	41.2 ± 0.1
15	2	2	3	1	3	40.8 ± 3.5
16	2	3	1	2	1	38.2 ± 1.2
17	2	3	1	2	2	33.3 ± 0.8
18	2	3	1	2	3	26.6 ± 1.2
19	3	1	3	2	1	48.6 ± 2.5
20	3	1	3	2	2	35.8 ± 2.7
21	3	1	3	2	3	35.7 ± 3.1
22	3	2	1	3	1	0
23	3	2	1	3	2	0
24	3	2	1	3	3	0
25	3	3	2	1	1	38.0 ± 1.1
26	3	3	2	1	2	21.9 ± 0.9
27	3	3	2	1	3	24.0 ± 1.5
H	1	3	3	2	1	50.9 ± 2.3

Data represent mean $\pm$ SD, $n = 3$.
Note: A, air flow; B, inlet temperature; C, aspirator%; D, pump rate; E, feed concentration. Numeric values 1–27 indicate experimental run number, H indicate optimum spray-drying condition that produce highest yield%.

Figure 3 presents the mean S/N graph of the yield % for each factor level. The factor with the largest range and corresponding rank (indicating the relative importance compared with other factors) was regarded as the significant factor influencing the yield %. Optimum specifications were determined by high S/N ratios. Based on the range, rank and S/N response graph, production of highest dry powder yield % according to the Taguchi's 'larger-is-better' criterion in Minitab 16 statistical software suggested combinations A1B3C3D2E1 (run H—Table 4). When run H was performed the dry powder yield % was 50.9 ± 2.3%.

Figure 4 represents the SEM photomicrographs of NCMPs and run H regarding the shape and surface morphology, which was irregular and porous microparticle carriers. The selected HDL NPs and SPS NPs were spray-dried using run H parameters (because it produced the highest yield% of powder ~50%) to produce NCMPs. The formulations were given the following
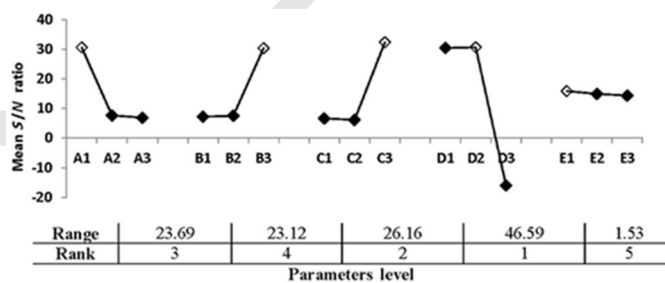
Figure 3. Mean signal-to-noise (S/N) graph for yield % response. Letters (A–E) indicate the experimental parameters and numeric value indicates the parameter levels, ◊ indicates maximum S/N value. A, airflow; B, inlet temperature; C, aspirator %; D, feed rate %; E, feed concentration.
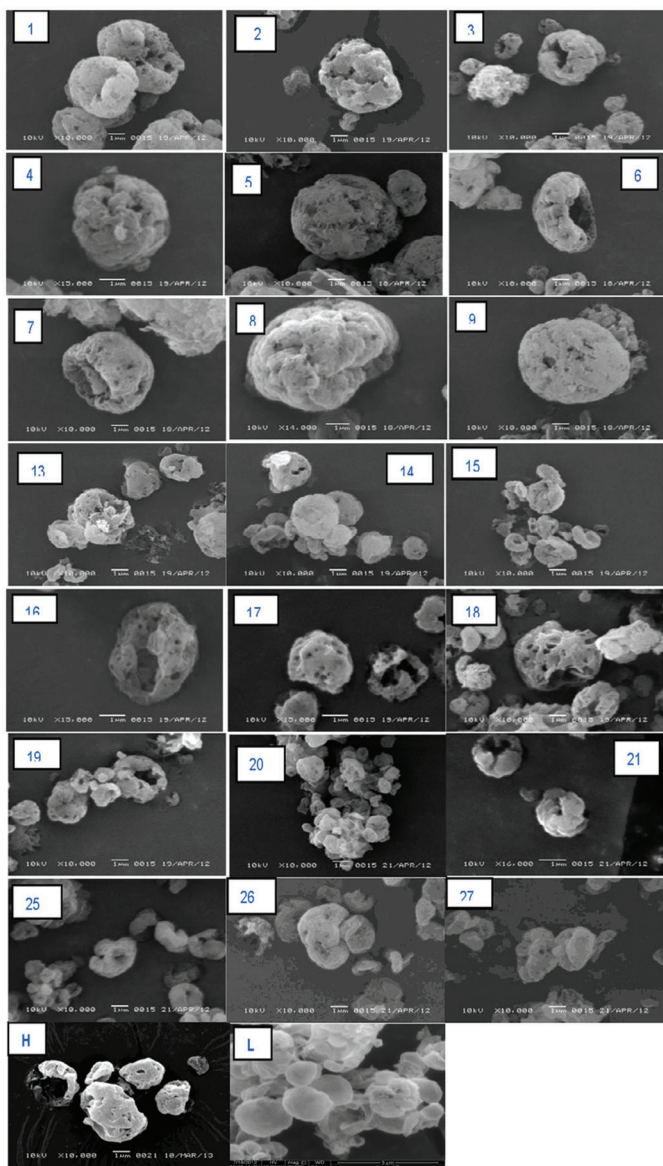
Figure 4. SEM images of NCMPs prepared by different spray-drying conditions (numeric values 1–27 indicates run experimental number, H: NCMPs spray-dried with run H (HDL H NCMPs), L: L-leucine alone spray-dried with run H. The scale bar represents 1 μm.

codes: HDL H NCMPs, and SPS H NCMPs. Formulations SPS H NCMPs and HDL H NCMPs were carried out for further investigations. The NCMPs had a residual moisture content of $0.2 \pm 0.03\%$ (w/w).

Primary Aerodynamic Diameter and In Vitro Aerosolisation Studies for NCMPs

There was no significant difference between NCMPs formulations regarding geometric particle size (HDL: 3.89 ± 0.37 and SPS: 4.69 ± 0.77 μm) ($p > 0.05$). However, significant difference ($p < 0.05$) was observed between the NCMPs formulations with respect to tapped density and carr's index. The theoretical aerodynamic diameter (d_{ae}) was calculated from both these parameters and ranged from 1.45 ± 0.14 and 1.71 ± 0.32 μm (Table 5) indicating the suitability for pulmonary delivery, but no signif-
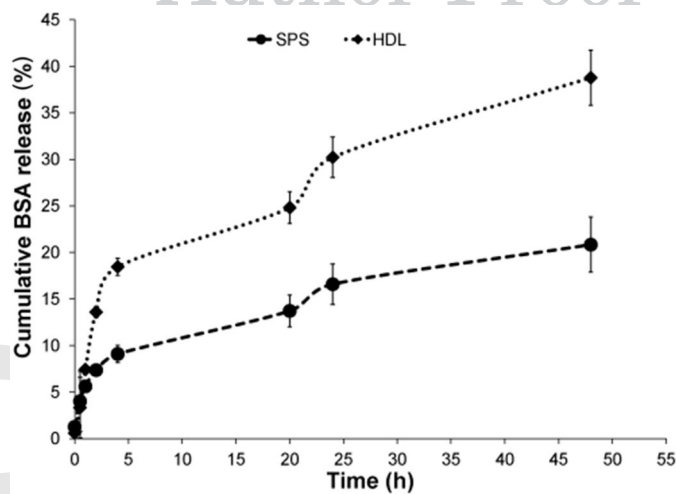
Figure 5. Cumulative *in vitro* release of BSA from NCMPs in PBS buffer at 37°C. (Data represent mean $\pm$ SD, $n = 3$.)

icant difference ($p ? 0.05$). BSA deposition data obtained from NCMPs (Table 6) indicated there was no significant difference in FPD and MMAD ($p ? 0.05$), but HDL H NCMPs achieved a significantly higher FPF ($p < 0.05$) between the formulations examined.

In Vitro Release Studies

In vitro release studies comparing SPS H NCMPs and HDL H NCMPs formulations were performed (Fig. 5) and showed a biphasic release profile. An initial burst release was observed up to 4 h with BSA release from HDL H NCMPs ($18.46 \pm 0.92\%$) significantly greater than SPS H NCMPs ($9.09 \pm 3.4\%$) ($p < 0.05$) followed by a continuous release over 48 h. A significant difference ($p < 0.05$) was noted in the release profile (24–48 h) between HDL H NCMPs and SPS H NCMPs, with HDL H NCMPs achieving $38.77 \pm 3\%$ release after 48 h compared with $20.84 \pm 4.2\%$ for SPS H NCMPs .

In this study, BSA was released from SPS H NCMPs and HDL H NCMPs following the Higuchi diffusion model ($r^2 = 0.981$ and 0.955, respectively) with a release rate constant (k_1, h$^{-\frac{1}{2}}$) of 2.7021 and 5.3653, respectively (Table 7). Hence, the release of BSA from NCMPs seems to be a diffusion-limited process. Accordingly HDL H NCMPs was selected for further investigation in this study.

Investigation of BSA Structure and Activity

The primary structure of BSA released from NPs and NCMPs was analysed by SDS-PAGE (Fig. 6). The BSA standard and molecular weight marker shown in lanes 1 and 5, respectively, revealed a clear band at about 66 kDa. The BSA released from HDL NPs (lane 2) and from HDL H NCMPs (lanes 3 and 4), showed similar clear banding patterns to the BSA standard (Fig. 6). The single lines in the gels provided evidence that the BSA released did not undergo significant covalent aggregation or fragmentation during the formulation methods used. The residual esterolytic activity of the BSA sample was evaluated to be $74.98 \pm 5.8\%$ relative to standard BSA.

The secondary structure of BSA was analysed using CD spectroscopy (Fig. 7). The structure of standard BSA and BSA released, indicated minima at 221–222 and 209–210 nm and a

Author Proof

Table 5. The Geometric Particle Size, Tapped Density and Theoretical Aerodynamic Diameter of Spray-Dried NCMPs

Formulation	Particle size (µm)	Tapped density (g/cm³)	Carr's Index		d_{ae} (µm)
			%	Flowability	
SPS H NCMPs	4.69 ± 0.77	$0.132 \pm 0.007^*$	$36.21 \pm 1.5^*$	Very poor	1.71 ± 0.32
HDL H NCMPs	3.89 ± 0.37	0.145 ± 0.002	31.25 ± 1.7	Poor	1.46 ± 0.14

Data represent mean $\pm$ SD, $n = 3$.
$^*p < 0.05$, ANOVA/Tukey's comparison.

Table 6. The Fine Particle Dose (FPD), Percentage Fine Particle Fraction (FPF) and Mass median Aerodynamic Diameter (MMAD) of NCMPs

Formulation	FPD (µg)	FPF (%)	MMAD (µm)
SPS H NCMPs	38.04 ± 2.80	$64.32 \pm 1.6^*$	1.49 ± 0.13
HDL H NCMPs	45.00 ± 7.40	78.57 ± 0.1	1.71 ± 0.10

Data represent mean $\pm$ SD, $n = 3$.
$^*p < 0.05$, ANOVA/Tukey's comparison.

Table 7. Release Parameters of BSA from NCMPs

Formulation	Zero Order		First Order		Higuchi	
	r^2	k_o (h⁻¹)	r^2	k_1 (h⁻¹)	r^2	k_1 (h⁻¹ᐟ²)
HDL H NCMPs	0.842	0.72	0.886	-0.004	0.955	5.3653
SPS H NCMPs	0.881	0.366	0.899	-0.0018	0.981	2.7021
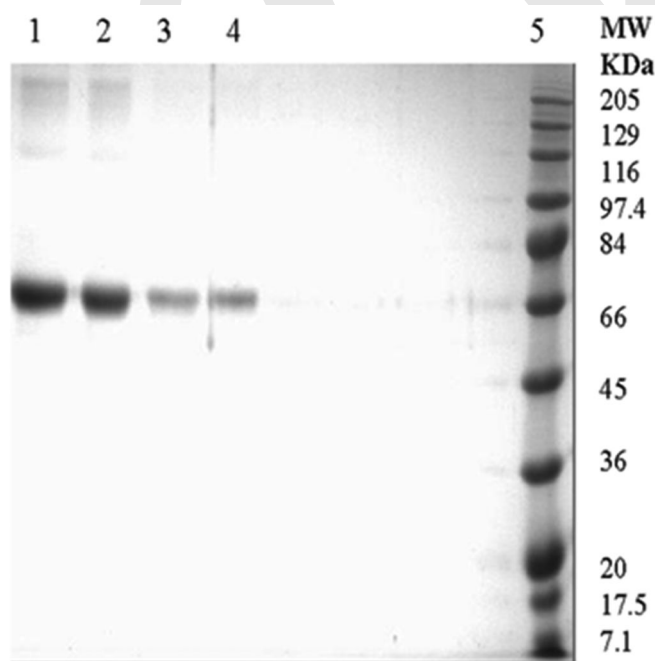
Figure 6. SDS-PAGE behaviour of BSA released for the assessment of BSA stability. Lanes represent, BSA standard (1), BSA released from HDL NPs (2), BSA released from HDL H NCMPs (3, 4), and molecular weight (MW) standard markers, BSA (MW 66,000), (5). Difference in band intensity was due to different loading.

Figure 7. The CD spectra of BSA released from HDL NPs (grey) and BSA standard (black).

maximum at 195 nm for both samples, which is typical for α-helical structure. In support of these data, structural analysis showed that BSA was predominantly helical displaying 51.5% helicity (Table 8), which is in good agreement with Zhang et al.[37] Structural analysis of BSA released displayed double minima at 210 and 222 nm and a further spectra analysis showed a reduced level of α-helical conformation (*circa* 48.5% helical) (Table 8). Furthermore, a comparison of BSA released with standard BSA showed that the α-helical content decreased by 3%.

Cell Viability Studies and NPs Cellular Uptake by DCs

The unloaded NPs and NCMPs appeared to be well tolerated by the A549 cell line, with a cell viability of $84.63 \pm 5\%$ for NPs and $75.7 \pm 4\%$ for NCMPs (Fig. 8) at 1.25 mg/mL concentration after 24 h exposure. In addition, the unloaded NPs displayed a cell viability of $86.38 \pm 5.5\%$ at 5 mg/mL concentration after 4 h exposure in DCs, indicating good cell viability with increasing NP concentration (Fig. 9).

Figure 10 shows the intracellular localisation of FITC-BSA-loaded NPs inside DCs after 4 h incubation. The cell wall of the DCs was stained with WGA TR, the nucleus was stained with DAPI and the NPs loaded with FITC-BSA were observed under red, blue and green channels, respectively. The green fluorescence was observed inside the DCs confirming the presence of NPs.

Table 8.   The Percentage of Secondary Structure Conformation for BSA Released from the Selected Formulation and BSA Standard

Sample	Helix	Strands	Turns	Unordered
BSA standard	51.5 ± 0.007	21.50 ± 0.007	9.0 ± 0	17.50 ± 0.007
BSA released	48.50 ± 0.007	25.0 ± 0	6.50 ± 0.007	19.5 ± 0.007

Data represent mean $\pm$ SD, $n = 3$.
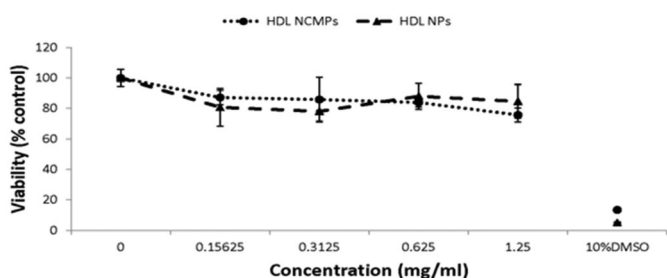
Figure 8.   A549 cell viability measured by MTT assay after 24 h exposure to NPs and NCMPs. (Data represent mean $\pm$ SD, $n = 3$.)
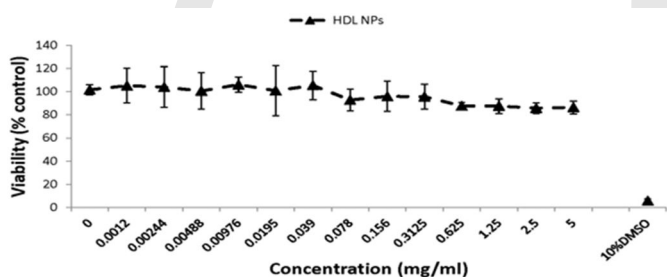
Figure 9.   DCs viability measured by MTT assay after 4 h exposure to NPs. (Data represent mean $\pm$ SD, $n = 3$).

DISCUSSION

Preparation and Characterisation of NPs

The loading capacity of NPs is a critical aspect for delivery as high loading results in greater bioavailability of drug per particle absorbed.[38] A successful drug delivery system should have a high loading capability which will decrease the amount of drug and excipients used for manufacturing the delivery system. Analysis of the results from the Taguchi design indicated that the DL of NPs was influenced by different parameters in the following order: BSA concentration > IAP volume > polymer mass > PVA concentration > OP volume > EAP sonication time and IAP sonication time > sonication amplitude; whereas the influence on the particle size of NPs had the following order: polymer mass > OP volume > sonication amplitude > surfactant concentration > EAP sonication time IAP sonication time > IAP volume > BSA concentration.

Bovine serum albumin concentration (rank 1; Fig. 2) had the greatest influence on the DL which increased profoundly as the BSA concentration increased from 0.2% to 1%. This was expected from predictions based on Eq. 1 in which DL is positively proportional to the amount of BSA[38] and can be seen comparing run 7 ($4.1 \pm 0.6\,\mu g/mg$) and run 18 ($15.7 \pm 4.8\,\mu g/mg$). However, increasing the BSA concentration to large levels (1%) is not necessarily beneficial; this trend has been explained by the mass of polymer used being insufficient to completely encapsulate the BSA.[38] Furthermore, higher concentrations of BSA provide a higher concentration in IAP droplets and thus increase the concentration gradient between the IAP droplets and the EAP, resulting in an increased amount of BSA transported into the EAP.[39,40] IAP volume (rank 2; Fig. 2) plays an important role on DL, such that, the larger volume of the IAP the higher the BSA loading, as seen in run 13 ($1.4 \pm 0.5\,\mu g/mg$) and run 19 ($5.0 \pm 0.1\,\mu g/mg$) (Table 3). This effect has been reported[38,41] and is thought to be due to a decrease in the concentration gradient between IAP and EAP.

The third factor affecting DL was the polymer mass (rank 3; Fig. 2). DL decreased substantially with increasing polymer mass from 50 to 200 mg, as predicted based on Eq. 1, in which DL is inversely proportional to the polymer mass.[42] This trend can be seen in run 22 ($5.6 \pm 0.04\,\mu g/mg$) and run 25 ($2.8 \pm 0.1\,\mu g/mg$). In addition, the results showed that reducing the OP volume (rank 5; Fig. 2) increased DL. This was associated with the high viscosity of the OP resulting in enhanced primary emulsion stabilisation and minimising the diffusion rate of BSA through the OP.[41]

The fourth factor affecting DL was PVA concentration, with 1% PVA resulting in higher BSA loading as seen comparing run 19 ($5.0 \pm 0.1\,\mu g/mg$) and run 22 ($5.6 \pm 0.04\,\mu g/mg$) (Fig. 2). A possible explanation was that at this concentration PVA was adequate to completely cover the partition interface (organic/aqueous) and subsequently resulting in reduced leaching of BSA. Consequently, any further increase in PVA concentration (5% and 10%) resulted in decreased DL because of the enhanced partitioning of BSA into the aqueous phase during emulsification. This was attributed to the solubilisation and emulsification effect of PVA.[43]

Sonication time of the EAP and IAP exerted similar effects on DL where increasing the sonication time of IAP and EAP resulted in higher DL.[44] The factor that had the least effect was sonication amplitude. Increasing the sonication amplitude (30% to 45% to 65%) had almost no beneficial effect on the BSA loading. This effect has been reported previously and has been associated with BSA precipitation within the sonication probe due to high pressure and increased fluid cavitations during sonication.[45,46]

Analysis of results following the Taguchi design indicated that the particle size of NPs was influenced by different parameters in the following order: polymer mass > OP volume > sonication amplitude > surfactant concentration > EAP sonication time and IAP sonication time > IAP volume > BSA concentration. It can be seen that the polymer mass followed by the OP volume (rank 1 and 2; Fig. 1) had the greatest effect on NPs size. An increase polymer mass resulted in an enhanced NP size, with run 3, 6, 9, 20 and 23 achieving the largest NPs size (Table 3). This was demonstrated by the observation that PGA-co-PDL mass was the primary parameter accountable for the variation in NPs size. A similar observation has also been noted by Bilati et al.[38] investigating PLGA NPs encapsulated
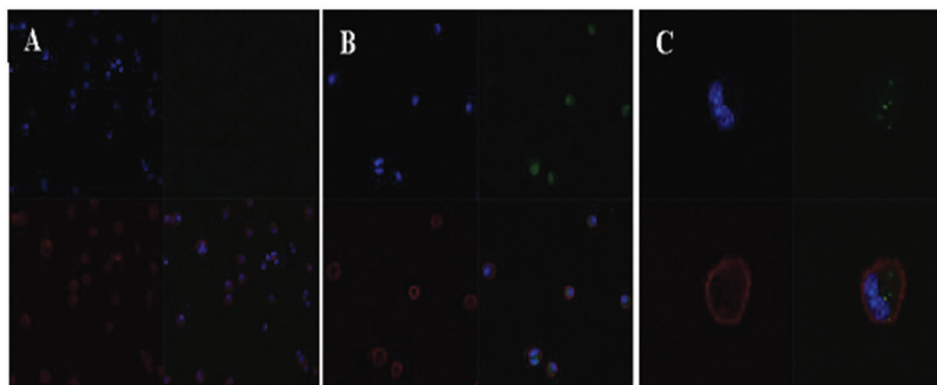
Figure 10. Confocal microscopic image of FITC-BSA NPs uptake by DCs. (a) DCs incubated without NPs at 20×, (b) DCs incubated with FITC-BSA NPs at 20×, (c) DCs incubated with FITC-BSA NPs at 63×, red channel for WGA TR, blue channel for DAPI and green channel for FITC-BSA.

with protein prepared using a double emulsion solvent evaporation method or with microparticles. The effect of polymer mass on the particle size has also been attributed to the increased viscosity and subsequent less proficient stirring of the OP leading to an greater NPs coalescence.[47]

Poly(vinyl alcohol) concentration was directly proportional to size with a trend of $1 < 5 < 10\%$ PVA (rank 4; Fig. 1). This was associated with an increase in viscosity with increase in PVA concentration in the IAP corresponding to a reduced shear stress, decreased diffusion rate and consequently increase in NP size. This can be seen comparing run 4 (1% PVA, 498.7 ± 4.6 nm) and run 7 (5% PVA, 577.8 ± 107.4 nm) (Table 3). Furthermore, additions of more PVA lead to an enlargement in NPs size because of the buildup of surplus molecules at the surface leading to bridging between the primary particles.[43] BSA concentration and IAP volume had minimum effect on the particle size of NPs which has also previously been reported in literature.[38]

The rate of size reduction decreased considerably when sonication was carried out beyond the duration of 5 s for IAP (rank 6) or 15 s for EAP (rank 5) or beyond the amplitude (rank 3) of 45% (Fig. 1). Increasing amplitude lead to more fluid cavitation, this inhibits the efficiency of energy transmission and decreased ultrasonic effect.[48] This can be seen in run 10 and 29 (Table 3) which differ in amplitude (65% and 45%, respectively), sonication time for IAP (10 and 15 s, respectively) and EAP (10 and 30 s, respectively)

Precise adjustment of the numerous formulation and processing factors is important to attain the desired NPs size and BSA loading. In this study, a particle size of ≤500 nm was desired to facilitate uptake of NPs by DCs.[6,7,49] A high S/N ratio suggested optimum conditions such that, the larger the S/N ratio, the less variance of particle size and BSA loading from the desired value. When the suggested optimized run was carried out, the measured particle size (SPS NPs) obtained 203 ± 5.4 nm was considered suitable for DCs uptake.[50–52]

NCMP Characterisation

Spray-drying was utilised to encompass the selected NPs into NCMPs with L-leucine as a carrier and to enhance powder dispersion. Majority of the spray-drying process parameters achieved low yields because of the condensation inside the drying chamber and collecting vessel resulting in the dry particles

sticking to the walls.[53] Utilising the Taguchi design revealed that the feed rate, aspirator capacity, air flow and inlet temperature had the greatest effects on the yield% of dry powder, whereas the change in the concentration of total solid in the spray-dried suspension had no effect in the yield% of dry powder.

The most important factor was feed rate (rank 1; Fig. 3) with a negative effect on powder yield. At high feed rates 15%, it is difficult for the atomized air to penetrate the liquid stream. Consequently, insufficient atomisation and drying will result with large NCMPs deposition and sticking to the walls in the drying and cyclone chambers.[53]

The second important factor was aspirator flow (rank 2; Fig. 3) with a positive effect on powder yield% (rank 2). A high aspirator flow rate created greater centrifugal force leading to an increase in the collection efficiency.[54] Airflow had a negative effect on powder yield% (rank 3; Fig. 3). Higher spray flow produced smaller droplets which were collected less efficiently by the centrifugal force in the cyclone.[54]

The inlet temperature (rank 4; Fig. 3) of drying air ranged from 50°C to 100°C, typically resulting in an outlet temperature of approximately 22°C to 46°C. It was noticed that as the inlet temperature increased from 50°C to 100°C there was an increase in powder yield%. It has been reported that a high inlet temperature can reduce the drying time and inhibit particle aggregation.[55] Furthermore, a higher inlet temperature promotes a decrease in residual moisture by enhancing water evaporation resulting in less particles sticking in the drying chamber.[56]

The results obtained from spray-drying regarding runs 10, 11, 12, 22, 23 and 24 produced no yield. They all shared the predominant factor (Feed Rate, rank 1; Fig. 3) affecting yield although they differed in other factors (aspirator capacity, air flow and inlet temperature) (Table 4). The feed rate was 15%, and at this high rate the atomising air may not be able to break the flow of the suspension. Furthermore, the high feed rate was accompanied by low level of aspirator capacity (50% and 75%), high level airflow (535 and 670 L/h) and low level of inlet temperature (50°C and 75°C), which all had negative effect on yield as explained above. When these parameters were adjusted to their positive level in run 7, 8 and 9 (Table 4) the yield increased up to 43%.

Author Proof

Photomicrographs showed irregular and porous NCMPs. This has been associated with vapour pressure that builds up during the removal of water throughout spray-drying and is prevalent with L-leucine and other hydrophobic amino acids, resulting in improved aerosolisation.[57] Furthermore, photomicrographs of NCMPs were similar irrespective of different processing conditions. High residual moisture content can promote particle aggregation leading to a variation in particle size distribution.[58] The low moisture content reported from the TGA thermogram presents a good drying efficiency therefore the dry powder formulations are likely to show good storage stability.

In Vitro Release and Aerosolisation Studies

Aerosolisation deposition data of NCMPs formulations indicated a similarity in FPD. The significantly higher FPF% of HDL H NCMPs compared with SPS H NCMPs was attributed to powder aggregation which was demonstrated by the large Carr's index, ≥32, implying the flow of SPS H NCMPs was very poor. In addition, SPS H NCMPs had a significantly smaller MMAD indicating possibility of aggregation and

In vitro release studies comparing SPS H NCMPs and HDL H NCMPs formulations were performed, with our results indicating a diffusion-limited process according to the Higuchi diffusion model. The observed change in release profile at 24 h following the initial burst release could be attributed to the distribution of BSA within NPs and/or alteration in degradation rate due to changed surface porosity.[24]

Stability of BSA and Cell Viability Studies

The primary structure of BSA released from HDL NPs and HDL H NCMPs showed similar clear banding patterns to the BSA standard provided evidence that the released BSA did not suffer significant covalent aggregation or fragmentation during the preparation methods used.

The secondary structure of BSA released was analysed using CD spectroscopy, a valuable technique in analysing the protein structure.[31] The spectra confirmed the presence of α-helix in the BSA released samples although this was decreased in comparison with standard BSA.

Bovine serum albumin has an enzyme-like activity and is able to hydrolyse substrates such as p-nitrophenyl esters.[36] When compared with standard BSA, the released BSA sample maintained approximately 74% of relative residual esterolytic activity, which was higher than 60% obtained by Abbate et al.[36] The reduction seen in this study was possibly due to the encapsulation process which resulted in a reduction in helicity as evaluated by CD (Fig. 7 and Table 8), and hence BSA activity. However, a 74% retention in activity achieved using this delivery system is still promising for further investigation of macromolecule delivery including proteins for vaccine.

The influence of NPs and NCMPs on cell viability studies were performed on the A549 and JAWS II DC lines. The NPs and NCMPs appear to be well tolerated by both cell lines. Although a decrease in cell viability was observed with increasing NPs and NCMPs concentration in both cell lines (A549: >75% at 1.25 mg/mL and DC: >85% at 5 mg/mL concentration), a high DL was obtained, which indicates lower doses could be delivered, hence negating the potential toxicity at high doses. Moreover, the dose delivered would be distributed throughout the lung and not localise within specific sites at these high concentrations.[59]

The uptake of NPs by JAWS II DC type was confirmed by CLSM. Thus NPs are efficiently ingested by DCs and could be applied for the delivery of antigens to DCs.

CONCLUSIONS Q5

The PGA-co-PDL NPs with appropriate size (203 ± 5.4 nm) to target DCs and BSA loading (43.67 ± 2.3 µg/mg) were successfully prepared using the Taguchi L36 orthogonal array design of experiment method. Selected NPs formulations were incorporated into NCMPs using L-leucine as a carrier. The highest yield% of dry powder (50%) was obtained using the Taguchi L27 orthogonal array design of experiment. The NCMPs had irregular and porous surface. The *in vitro* release studies indicated BSA maintains its primary and secondary structure. Furthermore, aerosolisation deposition data (FPF $78.57 \pm 0.1\%$ and MMAD 1.71 ± 0.1 µm) indicate deep lung deposition. In addition, the NPs and NCMPs had a relatively high cell viability (A549: >75% at 1.25 mg/mL and DC: >85% at 5 mg/mL concentration) at high concentrations. This study suggests that PGA-co-PDL NCMPs could be further investigated for pulmonary delivery of macromolecules, including the possibility for vaccine delivery via the pulmonary route.

REFERENCES

1. Reichert JM. 2003. Trends in development and approval times for new therapeutics in the United States. Nat Rev Drug Discov 2(9):695–702.

2. Kunda NK, Somavarapu S, Gordon SB, Hutcheon GA, Saleem IY. 2013. Nanocarriers targeting dendritic cells for pulmonary vaccine delivery. Pharm Res 30(2):325–341.

3. Sou T, Meeusen EN, de Veer M, Morton DA, Kaminskas LM, McIntosh MP. 2011. New developments in dry powder pulmonary vaccine delivery. Trends Biotechnol 29(4):191–198.

4. Pulliam B, Sung JC, Edwards DA. 2007. Design of nanoparticle-based dry powder pulmonary vaccines. Expert Opin Drug Deliv 4(6):651–663.

5. Rytting E, Nguyen J, Wang X, Kissel T. 2008. Biodegradable polymeric nanocarriers for pulmonary drug delivery. Expert Opin Drug Deliv 5(6):629–639.

6. Foged C, Brodin B, Frokjaer S, Sundblad A. 2005. Particle size and surface charge affect particle uptake by human dendritic cells in an in vitro model. Int J Pharm 298(2):315–322.

7. Kunda NK, Alfagih IM, Dennison SR, Tawfeek HM, Somavarapu S, Hutcheon GA, Saleem IY. 2015. Bovine serum albumin adsorbed PGA-co-PDL nanocarriers for vaccine delivery via dry powder inhalation. Pharm Res 32(4):1341–1353.

8. Kallinteri P, Higgins S, Hutcheon GA, St Pourcain CB, Garnett MC. 2005. Novel functionalized biodegradable polymers for nanoparticle drug delivery systems. Biomacromolecules 6(4):1885–1894.

9. Thompson CJ, Hansford D, Higgins S, Rostron C, Hutcheon GA, Munday DL. 2007. Evaluation of ibuprofen-loaded microspheres prepared from novel copolyesters. Int J Pharm 329(1–2):53–61.

10. Tawfeek H, Khidr S, Samy E, Ahmed S, Murphy M, Mohammed A, Shabir A, Hutcheon G, Saleem I. 2011. Poly(glycerol adipate-co-omega-

Author Proof

pentadecalactone) spray-dried microparticles as sustained release carriers for pulmonary delivery. Pharm Res 28(9):2086–2097.

11. Tawfeek HM, Evans AR, Iftikhar A, Mohammed AR, Shabir A, Somavarapu S, Hutcheon GA, Saleem IY. 2013. Dry powder inhalation of macromolecules using novel PEG-co-polyester microparticle carriers. Int J Pharm 441(1–2):611–619.

12. Lu D, Hickey AJ. 2007. Pulmonary vaccine delivery. Expert Rev Vaccines 6(2):213–226.

13. Stocke NA, Meenach SA, Arnold SM, Mansour HM, Hilt JZ. 2015. Formulation and characterization of inhalable magnetic nanocomposite microparticles (MnMs) for targeted pulmonary delivery via spray drying. Int J Pharm 479(2):320–328.

14. Ungaro F, d'Angelo I, Miro A, La Rotonda MI, Quaglia F. 2012. Engineered PLGA nano- and micro-carriers for pulmonary delivery: Challenges and promises. J Pharm Pharmacol 64(9):1217–1235.

15. Sinsuebpol C, Chatchawalsaisin J, Kulvanich P. 2013. Preparation and in vivo absorption evaluation of spray dried powders containing salmon calcitonin loaded chitosan nanoparticles for pulmonary delivery. Drug Des Devel Ther 7:861–873.

16. McBride AA, Price DN, Lamoureux LR, Elmaoued AA, Vargas JM, Adolphi NL, Muttil P. 2013. Preparation and characterization of novel magnetic nano-in-microparticles for site-specific pulmonary drug delivery. Mol Pharm 10(10):3574–3581.

17. Amaro MI, Tajber L, Corrigan OI, Healy AM. 2011. Optimisation of spray drying process conditions for sugar nanoporous microparticles (NPMPs) intended for inhalation. Int J Pharm 421(1):99–109.

18. Amaro MI, Tewes F, Gobbo O, Tajber L, Corrigan OI, Ehrhardt C, Healy AM. 2015. Formulation, stability and pharmacokinetics of sugar-based salmon calcitonin-loaded nanoporous/nanoparticulate microparticles (NPMPs) for inhalation. Int J Pharm 483(1–2):6–18.

19. Belotti S, Rossi A, Colombo P, Bettini R, Rekkas D, Politis S, Colombo G, Balducci AG, Buttini F. 2014. Spray dried amikacin powder for inhalation in cystic fibrosis patients: A quality by design approach for product construction. Int J Pharm 471(1–2):507–515.

20. Razavi Rohani SS, Abnous K, Tafaghodi M. 2014. Preparation and characterization of spray-dried powders intended for pulmonary delivery of insulin with regard to the selection of excipients. Int J Pharm 465(1–2):464–478.

21. Al-fagih I, Alanazi F, Hutcheon G, Saleem I. 2011. Recent Advances Using Supercritical Fluid Techniques for Pulmonary Administration of Macromolecules via Dry Powder Formulations. Drug Delivery Letters 1:128–134.

22. Li X, Vogt FG, Hayes D, Jr., Mansour HM. 2014. Design, characterization, and aerosol dispersion performance modeling of advanced co-spray dried antibiotics with mannitol as respirable microparticles/nanoparticles for targeted pulmonary delivery as dry powder inhalers. J Pharm Sci 103(9):2937–2949.

23. Osman R, Al Jamal KT, Kan PL, Awad G, Mortada N, El-Shamy AE, Alpar O. 2013. Inhalable DNase I microparticles engineered with biologically active excipients. Pulm Pharmacol Ther 26(6):700–709.

24. Jensen DM, Cun D, Maltesen MJ, Frokjaer S, Nielsen HM, Foged C. 2010. Spray drying of siRNA-containing PLGA nanoparticles intended for inhalation. J Control Release 142(1):138–145.

25. Yang SC, Zhu JB. 2002. Preparation and characterization of camptothecin solid lipid nanoparticles. Drug Dev Ind Pharm 28(3):265–274.

26. Lee SH, Heng D, Ng WK, Chan HK, Tan RB. 2011. Nano spray drying: A novel method for preparing protein nanoparticles for protein therapy. Int J Pharm 403(1–2):192–200.

27. Thompson CJ, Hansford D, Higgins S, Hutcheon GA, Rostron C, Munday DL. 2006. Enzymatic synthesis and evaluation of new novel ω-pentadecalactone polymers for the production of biodegradable microspheres. J Microencapsul 23(2):213–226.

28. Taguchi G, Yokoyama Y. 1993. Taguchi methods: Design of experiments. ASI Press.

29. Wong W, Crapper J, Chan HK, Traini D, Young PM. 2010. Pharmacopeial methodologies for determining aerodynamic mass distributions of ultra-high dose inhaler medicines. J Pharm Biomed Anal 51(4):853–857.

30. Myrdal PB, Yalkowsky SH. 2007. Solubilization of drugs in aqueous media. In Encyclopedia of pharmaceutical technology; Swarbrick J, Ed. 3rd ed. New York: Informa Health Care. p 3311.

31. Greenfield NJ. 2006. Using circular dichroism spectra to estimate protein secondary structure. Nat Protoc 1(6):2876–2890.

32. Henzler Wildman KA, Lee DK, Ramamoorthy A. 2003. Mechanism of lipid bilayer disruption by the human antimicrobial peptide, LL-37. Biochemistry 42(21):6545–6558.

33. Whitmore L, Woollett B, Miles AJ, Janes RW, Wallace BA. 2010. The protein circular dichroism data bank, a Web-based site for access to circular dichroism spectroscopic data. Structure 18(10):1267–1269.

34. Whitmore L, Wallace BA. 2004. DICHROWEB, an online server for protein secondary structure analyses from circular dichroism spectroscopic data. Nucleic Acids Res 32(Web Server issue):W668–673.

35. Whitmore L, Wallace BA. 2008. Protein secondary structure analyses from circular dichroism spectroscopy: Methods and reference databases. Biopolymers 89(5):392–400.

36. Abbate V, Kong X, Bansal SS. 2012. Photocrosslinked bovine serum albumin hydrogels with partial retention of esterase activity. Enzyme Microb Technol 50(2):130–136.

37. Zhang J, Ma X, Guo Y, Yang L, Shen Q, Wang H, Ma Z. 2010. Size-controllable preparation of bovine serum albumin-conjugated PbS nanoparticles. Mater Chem Phys 119(1–2):112–117.

38. Bilati U, Allemann E, Doelker E. 2005. Poly(D,L-lactide-co-glycolide) protein-loaded nanoparticles prepared by the double emulsion method–processing and formulation issues for enhanced entrapment efficiency. J Microencapsul 22(2):205–214.

39. Bittner B, Kissel T. 1999. Ultrasonic atomization for spray drying: A versatile technique for the preparation of protein loaded biodegradable microspheres. J Microencapsul 16(3):325–341.

40. Yang YY, Chung TS, Ng NP. 2001. Morphology, drug distribution, and in vitro release profiles of biodegradable polymeric microspheres containing protein fabricated by double-emulsion solvent extraction/evaporation method. Biomaterials 22(3):231–241.

41. Cun D, Jensen DK, Maltesen MJ, Bunker M, Whiteside P, Scurr D, Foged C, Nielsen HM. 2011. High loading efficiency and sustained release of siRNA encapsulated in PLGA nanoparticles: Quality by design optimization and characterization. Eur J Pharm Biopharm 77(1):26–35.

42. Brunner CT, Baran ET, Pinho ED, Reis RL, Neves NM. 2011. Performance of biodegradable microcapsules of poly(butylene succinate), poly(butylene succinate-co-adipate) and poly(butylene terephthalate-co-adipate) as drug encapsulation systems. Colloids Surf B Biointerfaces 84(2):498–507.

43. Sanad RA, Abdel Malak NS, El-Bayoomy TS, Badawi AA. 2010. Preparation and characterization of oxybenzone-loaded solid lipid nanoparticles (SLNs) with enhanced safety and sunscreening efficacy: SPF and UVA-PF. Drug Discov Ther 4(6):472–483.

44. Walter E, Moelling K, Pavlovic J, Merkle HP. 1999. Microencapsulation of DNA using poly(DL-lactide-co-glycolide): Stability issues and release characteristics. J Control Release 61(3):361–374.

45. Wischke C, Borchert HH. 2006. Influence of the primary emulsification procedure on the characteristics of small protein-loaded PLGA microparticles for antigen delivery. J Microencapsul 23(4):435–448.

46. Zhang JX, Chen D, Wang SJ, Zhu KJ. 2005. Optimizing double emulsion process to decrease the burst release of protein from biodegradable polymer microspheres. J Microencapsul 22(4):413–422.

47. Li X, Deng X, Yuan M, Xiong C, Huang Z, Zhang Y, Jia W. 1999. Investigation on process parameters involved in preparation of poly-DL-lactide-poly(ethylene glycol) microspheres containing Leptospira Interrogans antigens. Int J Pharm 178(2):245–255.

48. Tang ES, Huang M, Lim LY. 2003. Ultrasonication of chitosan and chitosan nanoparticles. Int J Pharm 265(1–2):103–114.

49. Slutter B, Bal S, Keijzer C, Mallants R, Hagenaars N, Que I, Kaijzel E, van Eden W, Augustijns P, Lowik C, Bouwstra J, Broere F, Jiskoot W. 2010. Nasal vaccination with N-trimethyl chitosan and PLGA based nanoparticles: Nanoparticle characteristics determine quality and strength of the antibody response in mice against the encapsu-

lated antigen. Vaccine 28(38):6282–6291.

50. Gutierro I, Hernandez RM, Igartua M, Gascon AR, Pedraz JL. 2002. Size dependent immune response after subcutaneous, oral and intranasal administration of BSA loaded nanospheres. Vaccine 21(1–2):67–77.

51. Shakweh M, Ponchel G, Fattal E. 2004. Particle uptake by Peyer's patches: A pathway for drug and vaccine delivery. Expert Opin Drug Deliv 1(1):141–163.

52. des Rieux A, Fievez V, Garinot M, Schneider YJ, Preat V. 2006. Nanoparticles as potential oral delivery systems of proteins and vaccines: A mechanistic approach. J Control Release 116(1):1–27.

53. Motlekar N. 2009. Optimization of experimental parameters for the production of LMWH-loaded polymeric microspheres. Drug Des Devel Ther 2:39–47.

54. Shi S, Hickey AJ. 2010. PLGA microparticles in respirable sizes enhance an in vitro T cell response to recombinant Mycobacterium tuberculosis antigen TB10.4-Ag85B. Pharm Res 27(2):350–360.

55. Mohajel N, Najafabadi AR, Azadmanesh K, Vatanara A, Moazeni E, Rahimi A, Gilani K. 2012. Optimization of a spray drying process to prepare dry powder microparticles containing plasmid nanocomplex. Int J Pharm 423(2):577–585.

56. Billon A, Bataille B, Cassanas G, Jacob M. 2000. Development of spray-dried acetaminophen microparticles using experimental designs. Int J Pharm 203(1–2):159–168.

57. Baras B, Benoit MA, Gillard J. 2000. Parameters influencing the antigen release from spray-dried poly(DL-lactide) microparticles. Int J Pharm 200(1):133–145.

58. Anish C, Upadhyay AK, Sehgal D, Panda AK. 2014. Influences of process and formulation parameters on powder flow properties and immunogenicity of spray dried polymer particles entrapping recombinant pneumococcal surface protein A. Int J Pharm 466(1–2):198–210.

59. Bhardwaj V, Ankola DD, Gupta SC, Schneider M, Lehr CM, Kumar MN. 2009. PLGA nanoparticles stabilized with cationic surfactant: Safety studies and application in oral delivery of paclitaxel to treat chemical-induced breast cancer in rat. Pharm Res 26(11):2495–2503.

Q1   AU: Please check the hierarchy of all section headings for correctness.

Q2   AU: Please give the following address information for the manufacturers BDH, Laboratory Supplies, Sigma–Aldrich, Gibco by Life Technologies, Fisher Scientific, Geneflow Limited, Biosera, American Type Culture Collection (ATCC), Invitrogen, Ltd., Minitab Inc., SIGMA Laborzentrifugen GmbH, Buchi Labortechnik, Malvern Instruments Ltd., Teva Pharma, Bio-Rad, Jasco, Epoch, BioTek Instruments Ltd. and Carl Zeiss: town, state (if applicable) and country.

Q3   AU: As the first section is Introduction and it has no subparts, kindly check and correct the citation of 'section 1.5.1' and replace it with full name of the section.

Q4   AU: 13,000 rpm: please replace this with the correct g value.

Q5   AU: Please check the section heading Conclusions for correctness.

Q6   AU: Please provide publisher location in Ref. 28.